Journal of The Electrochemical Society

Preparation of Cu-Sn Layers on Polymer Substrate by Reduction-Diffusion Method Using Ionic Liquid Baths

Kuniaki Murase, Akira Ito, Takashi Ichii and Hiroyuki Sugimura

J. Electrochem. Soc. 2011, Volume 158, Issue 6, Pages D335-D341.
doi: 10.1149/1.3573984

Email alerting service Receive free email alerts when new articles cite this article - sign up in the box at the top right corner of the article or click here

To subscribe to *Journal of The Electrochemical Society* go to:
http://jes.ecsdl.org/subscriptions

© 2011 ECS - The Electrochemical Society

Journal of The Electrochemical Society, **158** (6) D335-D341 (2011)
0013-4651/2011/158(6)/D335/7/$28.00 © The Electrochemical Society

Preparation of Cu-Sn Layers on Polymer Substrate by Reduction-Diffusion Method Using Ionic Liquid Baths

Kuniaki Murase,[*,z] Akira Ito, Takashi Ichii, and Hiroyuki Sugimura

Department of Materials Science and Engineering, Kyoto University, Sakyo-ku, Kyoto 606-8501, Japan

A novel metallization of non-conductive epoxy substrate with Cu-Sn "speculum alloy," or "white bronze," was performed through successive electrochemical processes: (*i*) conventional electroless deposition of pure Cu layer and (*ii*) subsequent electrochemical alloying of the resulting pure Cu layer with Sn using an ionic liquid bath at 150°C, a medium-low temperature. Availability of the Sn quasi-reference electrode for the alloying was verified, and the resulting compact and adhesive Cu-Sn layers, composed of Cu_6Sn_5 and/or Cu_3Sn intermetallic phases, were examined as an alternative to nickel plating. The abundance of the two intermetallic phases was found to be dependent on the alloying potential and duration, and was discussed in terms of alloy formation thermodynamics of the Cu-Sn system.
© 2011 The Electrochemical Society. [DOI: 10.1149/1.3573984] All rights reserved.

Manuscript submitted February 4, 2011; revised manuscript received March 9, 2011. Published April 12, 2011.

Electrodeposition, or electroplating, of metals using cathodic reduction of corresponding metal ions in a solution is a basic technology for thin-layer processing to add desired properties to materials. While the phenomenon is nowadays applied for microfabrication in the fields of electronics and micromachining, the preparation of decorative and/or protective coatings is still the major purpose for which electrodeposition technology is used. Not only single metals but also alloy coatings are prepared by electrodeposition because electrodeposited alloys usually have enhanced properties for a given application compared with metals in the pure state.[1] However, there are sometimes difficulties associated with stable process operation of alloy electrodeposition compared to the case of pure metal electrodeposition because the deposition baths contain more constituents: two or more metal salts, corresponding complex formers, buffering agents, and additives (*e.g.* brightener and leveler). This complexity of alloy electrodeposition baths can shorten the lifespan of the baths, and at the same time makes waste bath treatments complicated and energy-consuming even though electrodeposition is considered an environmentally-friendly technique for thin-layer processes.

As an alternative, we have been developing a reduction-diffusion (RD), or electrochemical alloying, method to form alloy layers using baths that each contain a single metal component.[2,3] By using this method, silver-white Cu-Sn alloy layers with composition 40–60 wt % Sn (*i.e.* 26–45 atom % Sn) called "speculum metal" or "white bronze" are obtained through two successive steps:[3] (*i*) conventional electrodeposition of a pure Cu layer from an aqueous $CuSO_4$–H_2SO_4 bath containing only Cu^{2+} ions as a metal component, followed by (*ii*) the RD alloying using an ionic liquid-based another bath containing Sn^{2+} ions. Here, the use of nonvolatile and nonflammable ionic liquid (IL) as a solvent renders it possible to raise the process temperature of RD alloying up to 150–190°C, medium-low temperatures, and to speed up the alloy layer growth compared to that in aqueous baths, which cannot be operated at temperatures above 100°C in an ambient atmosphere. Although this method consists of two steps, the use of two separate baths each containing a single-metal component will extend the lifespan of the baths and also make waste bath treatment simpler and easier.

More recently, we demonstrated and briefly reported, as a short communication,[4] that the Cu-Sn alloy metallization of an epoxy substrate was also feasible by using electroless Cu deposition for step (*i*) above. Since the Cu-Sn alloy layer is a promising alternative to an allergenic nickel underplating for decorative gold or chromium electroplating, the Cu-Sn metallization of such non-conductive polymer substrates also needs to be developed. In the present paper, we report a more detailed analysis of resulting Cu-Sn layers in order to thoroughly discuss the mechanism and thermodynamics of the Cu-Sn alloy formation, and to investigate some materials properties as an alternative to nickel coating. In addition, the electrochemical stability of pure Sn electrode was also examined to verify the validity of this electrode as a quasi-reference when employed in RD alloying.

Experimental

Preparation of electrolytic bath for alloying.—Ready-made hydrophobic IL, 1-ethyl-3-methylimidazolium bis[(trifluoromethyl)sulfonyl]amide (EMI-Tf_2N; note that the Tf_2N^- anion where $Tf = SO_2CF_3$ is sometimes described as $TFSA^-$ or $TFSI^-$), was purchased from Kanto Kagaku or Merck and used without further purification. Although another IL, trimethyl-*n*-hexylammonium bis[(trifluoromethyl)sulfonyl]amide, was tried previously,[2,3] we used the thermally more stable EMI-Tf_2N in the present study.[5] Tin(II) salt, $Sn(Tf_2N)_2$, having the same anion as the IL was prepared by the acid-base reaction of SnO (Nacalai Tesque) with bis[(trifluoromethyl)sulfonyl]-amine ($HNTf_2$; Fluka): $SnO + 2HNTf_2 \rightarrow Sn(Tf_2N)_2 + H_2O$. Here, powdery SnO was added to 1 mol dm^{-3} aqueous solution of $HNTf_2$ and allowed to react at 70°C for more than 2 h under a nitrogen purge. Unreacted SnO was then filtered off and the water was vaporized away at 120°C under a nitrogen atmosphere, yielding a white hydrated $Sn(Tf_2N)_2$, which was further dried at 120°C for 3 days in a vacuum dryer. Note that the resulting $Sn(Tf_2N)_2$ salt may contain residual water and/or $HNTf_2$. In the present RD process, however, these residues, if present, have an insignificant effect on the reduction of Sn^{2+} to Sn^0, since the potential of Sn^{2+}/Sn^0 redox couple (E_{Sn^{2+}/Sn^0}) is not that negative. We also expected that the most part of these volatile residues would spontaneously vaporize away when the bath for alloying (hereafter referred to as the "alloying bath") is operated at medium-low temperatures. To yield the alloying bath, the resulting $Sn(Tf_2N)_2$ salt was weighed and dissolved at 80°C into the EMI-Tf_2N in an open dry chamber (Daikin HRG-50A), in which the dew point was kept lower than −50°C; the Sn^{2+} ion concentration of the alloying bath was 0.05 mol dm^{-3}.

Cu substrate for alloying.—Unless otherwise noted, a thin layer of Cu (thickness, *ca.* 0.5 μm) electrolessly deposited on a heat-resistant high-T_g glass epoxy substrate using a conventional aqueous electroless plating bath (Okuno Chemical Ind., ATS Addcopper IW) was used as the Cu substrate for the RD alloying (see Figs. 3a and 3b). As a plastic substrate for decorative electroless plating, ABS (acrylonitrile-butadiene-styrene) resin is generally used; however, ABS, a thermoplastic resin, cannot be used for the RD process at medium-low temperatures. Since the glass epoxy substrate was provided as a copper foil-clad laminate (Hitachi Chemical MCL-E-679) for printed-circuit board manufacturing, the copper foil was first completely removed by dissolving it into an aqueous etchant

* Electrochemical Society Active Member.
z E-mail: murase.kuniaki.2n@kyoto-u.ac.jp

containing 200 g dm^{-3} $Na_2S_2O_8$ (sodium persulfate) and 10 g dm^{-3} H_2SO_4. In consequence, the resulting epoxy substrate before Cu electroless deposition already had a roughened surface. In some experiments, a Cu sheet (thickness, 0.5 mm) polished with a #2000 emery paper or a piece of the above copper foil-clad laminate (thickness of Cu foil, 18 μm) was used as needed for the RD alloying.

RD alloying of Cu substrate.—Although the alloying bath was prepared in a dry chamber, the Cu-Sn alloying experiments using the RD process were performed under atmospheric conditions (not in a dry chamber or a glove box). To avoid the oxidation of Sn^{2+} ions to tetravalent Sn(IV) state, however, the alloying bath was deaerated with nitrogen gas, while Tachikawa et al. reported that the oxidation of Sn(II) to Sn(IV) state does not take place within a wider electrochemical window of BMP-Tf_2N (BMP^+: 1-*n*-butyl-1-methylpyrrolidinium).[6] The alloying bath was thermostatted at 150°C unless otherwise noted, and was agitated at ~500 rpm using a magnetic stirring unit with a glass-coated stirring bar. Most alloying experiments were carried out using a potentiostatic method with a three-electrode configuration consisting of the above electroless Cu on epoxy substrate as a working electrode (*i.e.*, cathode for RD alloying), Sn sheet as a counter electrode (*i.e.*, anode for RD alloying), and Sn rod immersed into the same alloying bath as a quasi-reference electrode. While we employed a conventional set of potentiostat (Hokuto Denko HA-151) and coulometer (Hokuto Denko HF-201) for the alloying experiments, an integrated electrochemical analyzer (ALS/CHI model 660C) was utilized for the other electrochemical experiments such as polarization measurements.

Characterization of Cu-Sn layers.—The surface morphology and average composition of the resulting Cu-Sn layers were examined by scanning electron microscope (SEM, Keyence VE-7800) and associated energy dispersive X-ray spectrometer (EDX, EDAX Genesis 2000). A focused ion beam technique (FIB, JEOL JFIB-2300) using Ga-ion source was employed to prepare cross-sectional samples and to obtain their secondary electron images. X-ray diffraction (XRD) measurements for phase identification were carried out with a scan mode of 2θ-θ using a Rigaku RINT 2200 X-ray diffractometer fitted with a copper X-ray tube. To assess the colors of the layers objectively, optical reflection spectra were recorded with a UV-visible spectrometer (Hitachi U-3500) with integrating sphere. An X-ray photoelectron spectrometer (XPS, Kratos Analytical ESCA-3400) equipped with Mg-Kα irradiation (10 kV, 10 mA) and an Ar-ion sputtering system was used to examine the chemical state of Cu-Sn layers at the surface.

Results and Discussion

Potential stability of Sn electrode as a reference.—Unlike the cases of aqueous systems, quasi-reference electrodes, or pseudo-reference electrodes, are widely used for electrochemical measurements in non-aqueous systems like ILs. For ILs, a simple non-reactive Ag or Pt wire immersed in the same medium has commonly been used,[7] but there is no guarantee that the potentials of these electrodes have long-term stability. In particular, the Cu-Sn alloying in the present study requires rather strict potential control for more than 1 day; as hereinafter described, for example, to obtain Cu_6Sn_5 phase the alloying potential should be controlled at around +5 mV versus the equilibrium potential for Sn^{2+}/Sn couple for the alloying bath. In our previous studies on metal electrodeposition from IL-based deposition baths,[8–10] an I^-/I_3^- electrode was used where Pt wire was placed in the same IL (without metal salts) containing 60 mmol dm^{-3} (n-$C_3H_7)_4NI$ and 15 mmol dm^{-3} I_2. The I^-/I_3^- electrode is stable and reliable at room temperatures, but could not be so at medium-low temperatures because elemental iodine (I_2) existing in equilibrium can vaporize away at elevated temperatures. On the other hand, if the potential of an elemental Sn wire or Sn rod immersed in the alloying bath containing Sn^{2+} ions is stable and dominated by the redox $Sn^{2+} + 2e = Sn$ then the Sn rod electrode will be a useful 'reference electrode of the first kind'[7] for the present RD alloying. Recently, Tachikawa et al. reported that the Sn^{2+}/Sn redox couple in BMP-Tf_2N is more reversible than other M^{2+}/M (M = Mn, Fe, Co, and Zn) couples,[6] suggesting that the Sn^{2+}/Sn redox is applicable for reference.

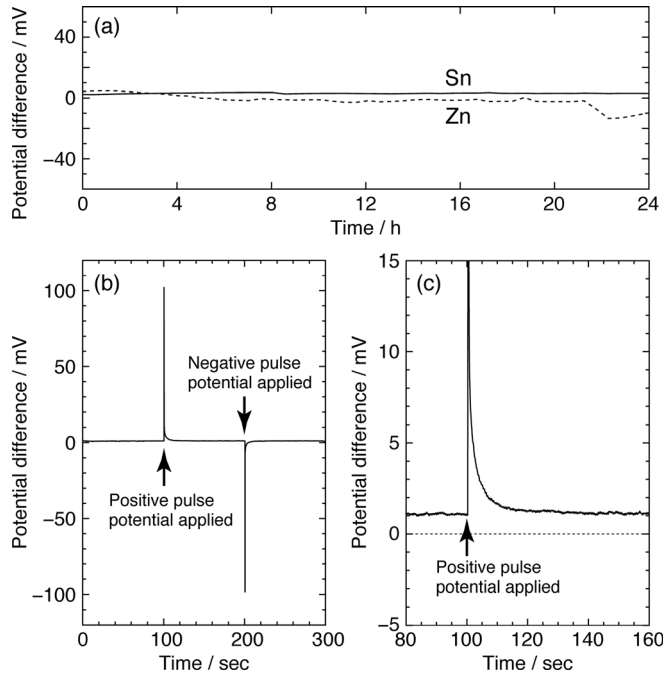

Figure 1. (a) Change in potential difference between two Sn electrodes or two Zn electrodes immersed in EMI-Tf_2N bath at 150°C containing 0.05 mol dm^{-3} $Sn(Tf_2N)_2$ or $Zn(Tf_2N)_2$ and (b, c) change in open-circuit potential of Sn electrode immersed in EMI-Tf_2N at 150°C containing 0.05 mol dm^{-3} $Sn(Tf_2N)_2$ when potential pulses of +100 and −100 mV *vs*. Sn rod were applied at times of 100 and 200 s, respectively.

To explore the availability of the Sn rod electrode, we performed several preliminary experiments. We assembled a three-electrode cell where the working, counter, and reference electrodes were all Sn rods immersed in the same alloying bath, *i.e.* EMI-Tf_2N containing 0.05 mol dm^{-3} $Sn(Tf_2N)_2$ at 150°C. Figure 1a shows the time variation in open-circuit potential, that is, the potential difference between two Sn rods placed in the same bath. Although the potential difference was not zero, the value was always fairly small, *i.e.*, about 2 mV in this case, and almost constant for 1 day or more, indicating long-term stability of the Sn rod electrode. An analogous experiment carried out for comparison using a couple of Zn electrodes placed in EMI-Tf_2N containing 0.05 mol dm^{-3} $Zn(Tf_2N)_2$ at 150°C exhibited a more fluctuating potential difference. We then tried to apply potential pulses of +100 and −100 mV *vs*. Sn rod, and the subsequent transient change in the open-circuit potential was monitored. As shown in Figs. 1b and 1c, the open-circuit potential after each pulse returned to the original value within 20 s, substantiating that the immersion potential of Sn electrode is stable against external electrical disturbance as is always required for a reference electrode. The immersion potential of the Sn rod at 50°C was −0.12 ± 0.01 V *vs*. I^-/I_3^-, which corresponds to −0.27 ± 0.01 *vs*. ferrocenium/ferrocene (Fc^+/Fc) couple.[8]

Following the results of verification, we measured a set of anodic and cathodic polarization curves and also carried out potentiostatic electrolysis at five different potentials: +15, +5, −5, −10, and −20 mV *vs*. Sn rod using the above three-electrode configuration. Figure 2a shows the current density during the potentiostatic electrolysis for 2 h. Even under these relatively small polarizations a set of constant anodic (at +15 and +5 mV) or cathodic (at −5, −10, and −20 mV) currents were observed, and the absolute value of the current increased with increasing polarization. The weight changes

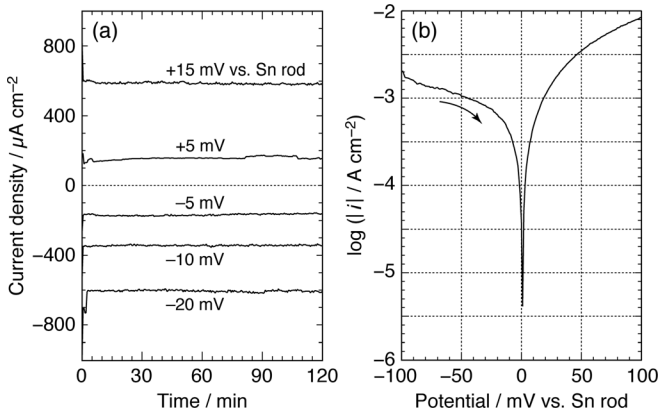

Figure 2. (a) Change in current density during potentiostatic electrolysis of Sn electrode at five different potentials and (b) polarization curves for Sn electrode with scan rate of 1 mV s^{-1}. Electrolyte was EMI-Tf_2N at 150°C containing 0.05 mol dm^{-3} $Sn(Tf_2N)_2$.

of Sn working electrodes after each electrolysis provided the evidence of anodic dissolution ($Sn \rightarrow Sn^{2+} + 2e$) or cathodic deposition ($Sn^{2+} + 2e \rightarrow Sn$) under the anodic and cathodic polarization, respectively, indicating that the open-circuit potential of the Sn electrode is really dominated by the redox: $Sn^{2+} + 2e = Sn$. We also confirmed that the current efficiency for the cathodic Sn deposition at − 10 and − 20 mV was 100%. Figure 2b depicts the polarization curves in Tafel form, which have a similar profile to those reported by Martindale et al.[11] for $Sn(Tf_2N)_2$ in BMP-Tf_2N, a hydrophobic Tf_2N^--based IL. While the curves did not have clearly straight Tafel segments, the apparent exchange current density for the Sn^{2+}/Sn redox roughly estimated using a tangent line at + 100 mV is in the order of 10^{-3} mA cm^{-2}.

Potential dependent RD alloying.—In response to the above results, we performed a series of potentiostatic RD alloying experiments using the Sn rod as a reference electrode. After the RD alloying for 72 h at + 5, + 10, and + 20 mV *vs*. Sn rod, a compact silver-white or silver-gray Cu-Sn alloy layer was obtained on the part immersed in the alloying bath, while the alloying at + 40 mV gave a charcoal gray layer. Currents during the alloying decayed slowly with time (data not shown) as we previously reported for the alloying using TMHA-Tf_2N bath.[2,3] When compared at a given time point, the current decreased with increasing alloying potential, *i.e*. with decreasing overpotential for reduction. Figure 3 shows the appearance and SEM images of the resulting layers, also depicting the images of the Cu layer before alloying (Fig. 3b) and the epoxy substrate (Fig. 3a). Owing to the roughened surface of the epoxy substrate, adhesions of the resulting Cu-Sn layers were good due to an anchoring effect, and the layers could not be peeled off with a standard Scotch® adhesive tape. The surface morphology of the Cu-Sn layers was similar to that of the initial Cu layer, reflecting the mechanism of RD alloying where the alloy grows by inward diffusion of Sn atoms from the surface toward the interior without formation of bulk Sn phase. In consequence, surface morphological evolution like dendrite or nodule formation unrelated to the initial Cu surface was not recognized on the surface. Figure 4 shows a set of cross-sectional secondary electron images of initial Cu and the resulting Cu-Sn layers alloyed at + 5 and + 20 mV. As is often the case with electroless plating, the initial Cu was conformally grown on the roughened epoxy substrate. While the resulting Cu-Sn layers

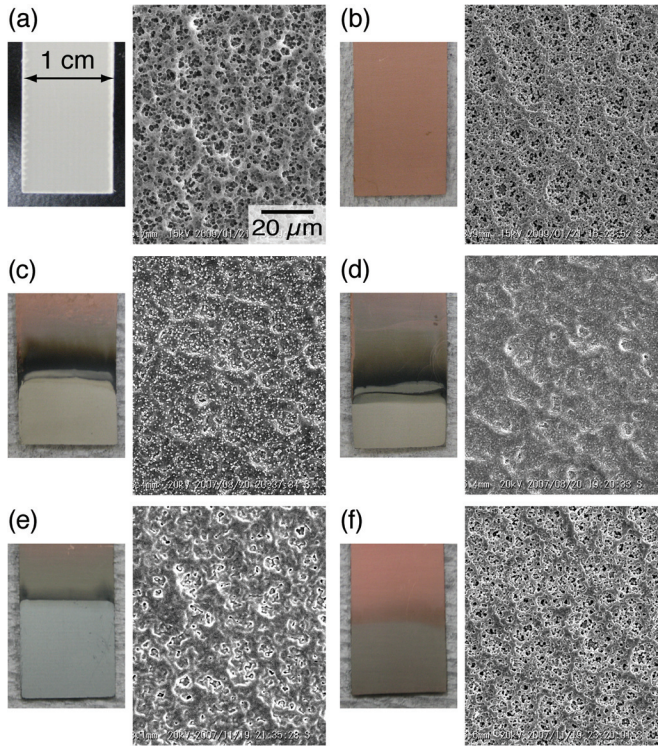

Figure 3. (Color online) Appearance and plan-view SEM images of (a) heat-resistant epoxy substrate, (b) electroless Cu layer on the substrate, and (c–f) Cu-Sn layers prepared by potentiostatic alloying for 72 h at 150°C using EMI-Tf_2N bath containing 0.05 mol dm^{-3} $Sn(Tf_2N)_2$. Alloying potentials were (c) + 5 mV, (d) + 10 mV, (e) + 20 mV, and (f) + 40 mV *vs*. Sn rod.

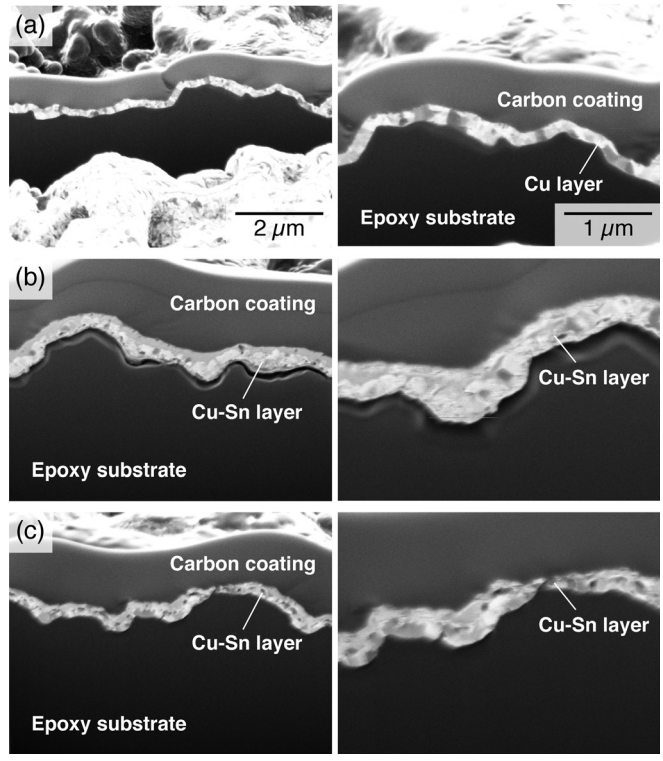

Figure 4. Cross-sectional secondary electron images of (a) electroless Cu layer on heat-resistant epoxy substrate and (b, c) Cu-Sn layers prepared by potentiostatic alloying for 72 h at 150°C using EMI-Tf_2N bath containing 0.05 mol dm^{-3} $Sn(Tf_2N)_2$. Alloying potentials were (b) + 5 mV and (c) + 20 mV *vs*. Sn rod. Images were taken at 60° tilted to the surface normal. Images on the right side are enlargements of those on the left.

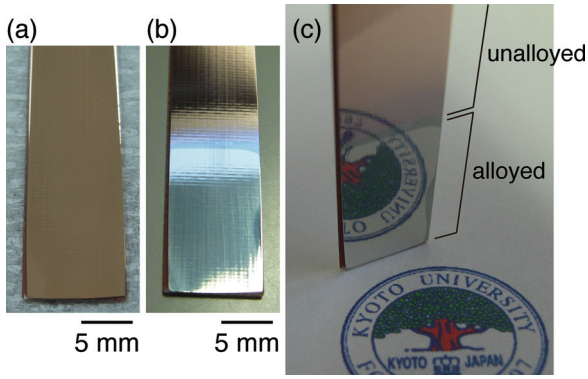

Figure 5. (Color online) Appearance of glossy Cu foil-clad laminate (a) before and (b, c) after potentiostatic alloying for 72 h at 5 mV *vs*. Sn rod and 150°C using EMI-Tf_2N bath containing 0.05 mol dm^{-3} $Sn(Tf_2N)_2$.

apparently kept the initial uniformity, a second look confirms that concave portions of the initial layer grew somewhat thicker than convex portions. This also reflects the mechanism of RD alloying where the total amount of Sn atoms introduced is not governed by the surface area but determined by the stoichiometry, that is the amount of initial Cu atoms. As described later, the main Cu-Sn phases obtained at +5 and +20 mV were Cu_6Sn_5 and Cu_3Sn, respectively, hence the former layer is thicker than the latter.

Since the initial Cu surface was rather rough (Fig. 4) with a matte appearance, all the resulting Cu-Sn layers were also lusterless (Fig. 3). In contrast, the alloying of glossy Cu foil-clad laminate under the same conditions (*i.e.* +5 mV) gave a lustrous Cu-Sn surface as shown in Fig. 5, also indicating that the initial Cu surface is a key to obtaining a flat and smooth speculum layer. In other words, as long as a lustrous Cu layer is prepared on a resin substrate using any well-established technique, the subsequent alloying bath does not always have to contain brightening and/or leveling agents as additives.

Figure 6 shows XRD patterns for the same samples as in Fig. 3. On the phase diagram of the Cu-Sn binary system, the thermodynamically stable Cu-Sn intermetallic phases at 150°C are η′-Cu_6Sn_5 (*ca*. 45 atom % Sn) and ε-Cu_3Sn (24.5–25.9 atom % Sn).[12] The layers alloyed at +5 and +20 mV were single-phase Cu_6Sn_5 and Cu_3Sn, respectively, while the layer obtained at +10 mV was a mixture of these two phases. These layers gave no diffraction of α-Cu (*i.e.* elemental fcc-Cu) or α-Cu(Sn) phase (*i.e.* fcc-Cu dissolving Sn atoms as a solid solution), indicating that all the initial Cu layers were converted to Cu-Sn alloys. In addition, diffraction due to β-Sn phase (*i.e.* elemental Sn), was also not found, since the alloying potentials are positive than 0 mV *vs*. Sn rod. We also confirmed by XRD that electrolysis at a slightly negative potential, −5 mV, really gave a pure β-Sn phase on the Cu substrate (data not shown). The potential-dependent alloy formation was also supported by a set of gross composition data from EDX analysis: The compositions of the layers prepared at +5, +10, and +20 mV were 45.9, 40.7, and 26.6 atom % Sn, respectively. In other words, Sn-rich phase, *i.e.* Cu_6Sn_5, whose tin activity a_{Sn} is higher than Cu_3Sn, was obtained at relatively low potential, while a lower a_{Sn} phase, *i.e.* Cu_3Sn, was formed at higher potentials. Unlike the cases of +5 to +20 mV, the main phase obtained at +40 mV was α-Cu(Sn) phase (Fig. 6f) containing 2.4 atom % Sn, probably due to the lack of time for sufficient alloying. As discussed later, the thermodynamically stable phase at +40 mV is Cu_3Sn.

Thermodynamics and growth mechanism.—To gain thermodynamic insight into the dependence of the alloying potentials on the formation of intermetallic phases, the thermodynamically stable phase for a given electrode potential was calculated as we previously reported for Cu-Sn alloying with a TMHA-Tf_2N bath at 130°C.[3] Here, we used literature data of Gibbs energy of formation[13]

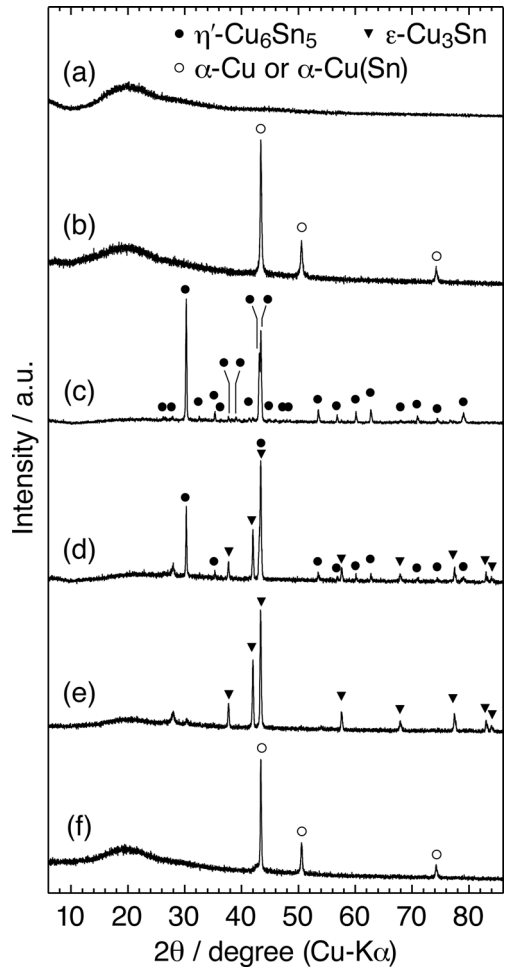

Figure 6. X-ray diffraction patterns of the same samples as in Fig. 3.

$$3Cu + Sn = Cu_3Sn \quad G^\circ_{Cu_3Sn}(J\,mol^{-1}) = -32776.8 - 0.8172T \quad [1]$$

$$6Cu + 5Sn = Cu_6Sn_5 \quad G^\circ_{Cu_6Sn_5}(J\,mol^{-1}) = -78426.7 + 4.4649T \quad [2]$$

where T is the absolute temperature, and considered four stable phases, *i.e.* β-Sn, Cu_6Sn_5, Cu_3Sn, and α-Cu(Sn). Figure 7 depicts the activity of tin (a_{Sn}) at 150°C (T = 423 K) as a function of tin content. The Nernst equation for $Sn^{2+} + 2e = Sn^0$ redox is given by

$$E_{Sn^{2+}/Sn^0} = E^\circ_{Sn^{2+}/Sn^0} - \frac{RT}{2F}\ln\frac{a_{Sn}}{a_{Sn^{2+}}} \quad [3]$$

where $a_{Sn}{}^{2+}$ is the activity of Sn^{2+} ions in the alloying bath; the other symbols E, E°, R, and F have the usual meanings. Note that Sn^0 stands for zero-valent tin including both elemental Sn and tin in Cu-Sn alloys. Since a_{Sn} of elemental Sn is 1 by convention, the immersion potential of the Sn rod reference electrode is

$$E_{Sn^{2+}/Sn^0} = E^\circ_{Sn^{2+}/Sn^0} - \frac{RT}{2F}\ln\frac{1}{a_{Sn^{2+}}} \equiv 0 \text{ } vs. \text{ Sn rod} \quad [4]$$

given that the immersion potential of Sn rod is dominated by $Sn^{2+} + 2e = Sn$ redox, and hence the deposition of pure Sn takes place at potentials negative to the immersion potential. In contrast, since a_{Sn} of Cu-Sn alloys is less than unity ($a_{Sn} < 1$), Cu-Sn alloys forms without codeposition of pure Sn at positive potentials as

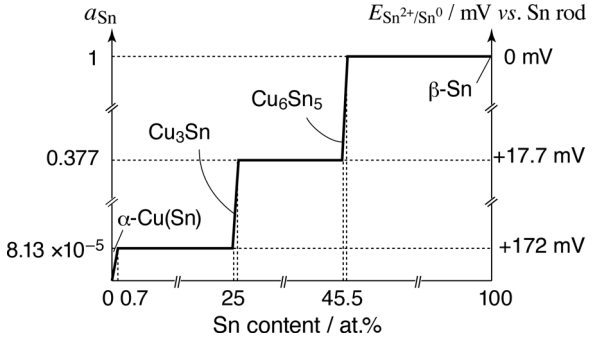

Figure 7. Activity of tin a_{Sn} and corresponding redox potential E_{Sn^{2+}/Sn^0} *vs.* Sn rod as a function of tin content of Cu-Sn alloys calculated using thermochemical data for Cu_6Sn_5 and Cu_3Sn intermetallic phases.

described in the preceding section. According to Eqs. 3 and 4, the potential E_{Sn^{2+}/Sn^0} for alloy formation with reference to the Sn rod electrode is

$$E_{Sn^{2+}/Sn^0}\ (vs.\ \text{Sn rod}) = -\frac{RT}{2F}\ln a_{Sn} \qquad [5]$$

The right ordinate of Fig. 7 is the potential E_{Sn^{2+}/Sn^0} corresponding to a_{Sn} values. The important thing is that, so long as the Sn rod electrode is employed and works properly, neither the activity of Sn^{2+} ions ($a_{Sn^{2+}}$) nor the solvent used for the alloying, governs E_{Sn^{2+}/Sn^0} (*vs.* Sn rod) values.

Figure 7 indicates that Cu_6Sn_5, Cu_3Sn, and α-Cu(Sn) phases are thermodynamically stable in the potential ranges $0 < E_{Sn^{2+}/Sn^0} < +17.7$ mV, $+17.7 < E_{Sn^{2+}/Sn^0} < +172$ mV, and $E_{Sn^{2+}/Sn^0} > +172$ mV, respectively. Thus the experimentally obtained phases, Cu_6Sn_5 at $+5$ mV and Cu_3Sn at $+20$ mV, were well accounted for by the thermodynamics. Meanwhile, the resulting alloy at $+10$ mV was a mixture of Cu_6Sn_5 and Cu_3Sn, although a single-phase Cu_6Sn_5 is thermodynamically expected. The reason for the discrepancy is unclear, but we think that it is due to a kinetic factor of the alloying, like the case of alloying at $+40$ mV, where α-Cu(Sn) phase formed in spite of the expected phase, *i.e.* Cu_3Sn.

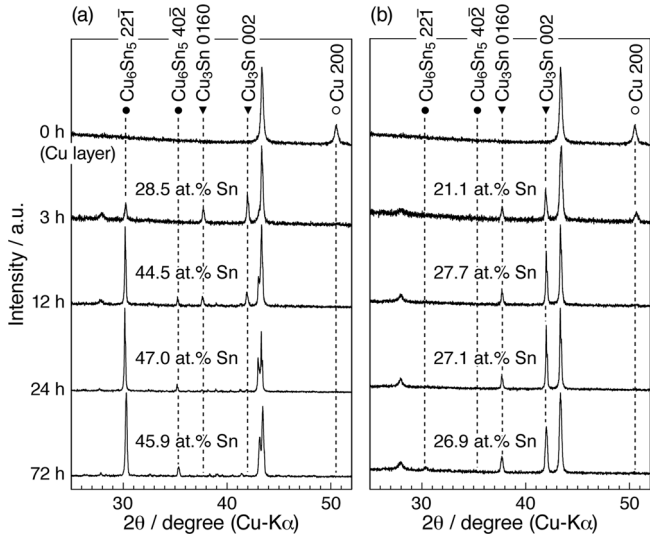

Figure 8. X-ray diffraction patterns and gross compositions of Cu thin layers before and after alloying for 3–72 h at 150°C using EMI-Tf_2N bath containing 0.05 mol dm^{-3} $Sn(Tf_2N)_2$. Alloying potentials were (a) $+5$ mV and (b) $+20$ mV *vs.* Sn rod. Indices of diffraction lines are based on JCPDS No. 45-1488 (Cu_6Sn_5), 01-1488 (Cu_3Sn), and 04-0836 (Cu).

In order to understand the alloy formation process in more detail, the change in phase during the alloying for 72 h was examined for two alloying potentials, $+5$ and $+20$ mV; Fig. 8 shows the changes in XRD patterns and gross compositions determined by EDX. At $+5$ mV, Cu_6Sn_5 phase appeared throughout the alloying for 72 h, while in the primary step of 3–12 h alloying Cu_3Sn phases were *also* recognized. In contrast, at $+20$ mV, only Cu_3Sn phase was formed throughout the alloying for 72 h. Based on the above thermodynamic discussion, it is reasonable that, at $+20$ mV, Cu_3Sn compound is initially formed on the surface and grows into the substrate by the diffusion of resulting Sn atoms until the whole Cu substrate is converted to single-phase Cu_3Sn. Similarly, at $+5$ mV, Cu_6Sn_5 compound is preferentially formed on the uppermost surface, but in this case Cu_3Sn compound is also formed at the boundary between the surface Cu_6Sn_5 layer and the unalloyed Cu underneath by a reaction diffusion in the Cu-Sn system. The entire Cu substrate is converted to single-phase Cu_6Sn_5 that is thermodynamically stable at $+5$ mV if a sufficient amount of tin atoms are supplied and enough time passes for them to diffuse into the substrate. Otherwise the Cu_3Sn phase remains and the resulting alloy layer is composed of Cu_6Sn_5 and Cu_3Sn, like the case of the alloying at $+10$ mV. Figure 9 gives the cross sectional SEM image and the profile of EDX line analysis for the Cu-Sn layer. Here, we used a polished Cu sheet (thickness, 0.5 mm) as a starting Cu substrate and the alloying was carried out for 72 h with a galvanic contact method at 190°C, a higher temperature, to accelerate the diffusion. In the galvanic contact method, the potential of the cathode during the alloying is spontaneously kept at around $+2$ to $+5$ mV,[2] which thermodynamically should result in the formation of Cu_6Sn_5 phase. The resulting Cu-Sn layer at the surface of the Cu sheet had a clear

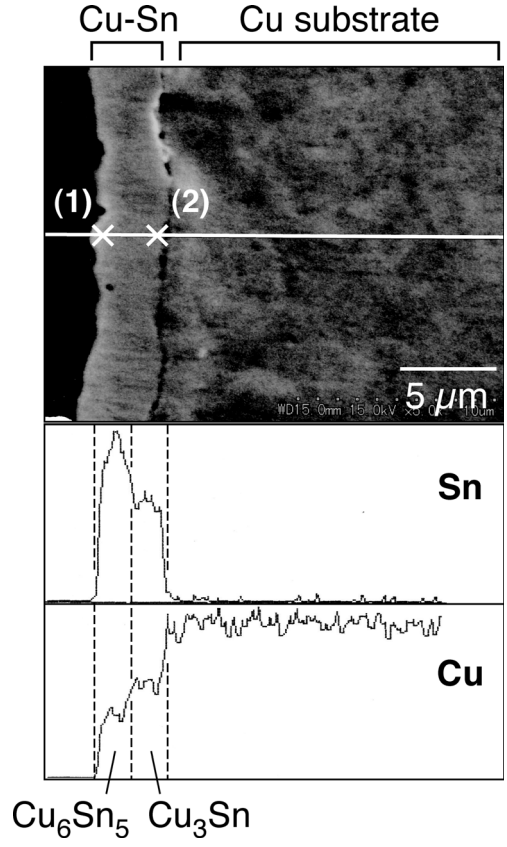

Figure 9. SEM image and EDX line profile of the cross-section of Cu-Sn layer grown on a Cu sheet by galvanic contact alloying for 72 h at 150°C using EMI-Tf_2N bath containing 0.05 mol dm^{-3} $Sn(Tf_2N)_2$. EDX point analysis data for outer and inner parts are (1) 46 atom % Sn and (2) 26 atom % Sn.

composition difference; the outer parts of the layer had compositions corresponding to Cu_6Sn_5 (Sn-rich) phase and the inner parts were Cu_3Sn (Cu-rich) phase. In other words, a Cu-rich Cu_3Sn phase is located between the substrate Cu and Sn-rich Cu_6Sn_5 phase. The presence of such a composition gradient also supports that the Cu-Sn layers are really grown by interdiffusion of Cu and Sn atoms. In any case, Fig. 8 indicates that the alloying of Cu substrate (thickness, *ca.* 0.5 μm) at + 5 and + 20 mV completed within 24 h.

Materials properties of single-phase Cu_6Sn_5 and Cu_3Sn layers.— The Cu-Sn phase diagram[12] indicates that, upon cooling of a Cu-Sn melt containing 45.5 atom % Sn, Cu_6Sn_5 phase (η phase) forms through a peritectic reaction between Cu_3Sn phase (ε phase) and the liquid phase, implying difficulty in the preparation of single-phase Cu_6Sn_5 by a simple fusion method. While aqueous alloy electrodeposition can prepare almost-single-phase Cu_6Sn_5,[14] the electrodeposition of single-phase Cu_3Sn has not been achieved to date. In contrast, our RD alloying can easily create both Cu_6Sn_5 and Cu_3Sn single-phases using potential and time control, and therefore it will be a useful tool for comparing the various physicochemical properties of these single-phase layers. In this study, differences in color and anodic property, as important surface properties when using the Cu-Sn layer for the underplating, were examined. The visible reflection spectra of Cu_6Sn_5 and Cu_3Sn layers prepared at + 5 and + 20 mV are shown in Fig. 10 together with spectra of the surfaces of Ni, Cu, and Ag sheets for comparison. As shown in Fig. 3, both Cu_6Sn_5 and Cu_3Sn layers were silver-white or silver-gray, but the Cu_3Sn layer looked somewhat bluish. In fact, their reflection spectra gave different profiles, accounting for the difference in color of each layer. The reflectance of the Cu_6Sn_5 layer gradually and monotonically increased with increasing wavelength like Ni and Ag, while that of Cu_3Sn had a local minimum at around 680 nm, of which the complementary color is blue-green. The important point is that the spectrum for the Cu_6Sn_5 layer resembles that for Ni. As noted in the Introduction, a "speculum metal" layer with 40–60 wt % Sn is anticipated as an alternative to nickel underplating, and one reason for this is that the Cu-Sn alloy has a pleasing silver-white color like nickel which enhances the brightness of, for example, gold plating over it. According to the Cu-Sn phase diagram,[12] the alloy of 40–60 wt % Sn generally consists of two phases, Cu_6Sn_5 and Cu_3Sn. The above result indicates the nickel-like color is mainly due to the *presence* of Cu_6Sn_5 intermetallic phase rather than Cu_3Sn phase; the mixed layer comprising Cu_6Sn_5 phase obtained at + 10 mV also has a nickel-like color without bluish coloring.

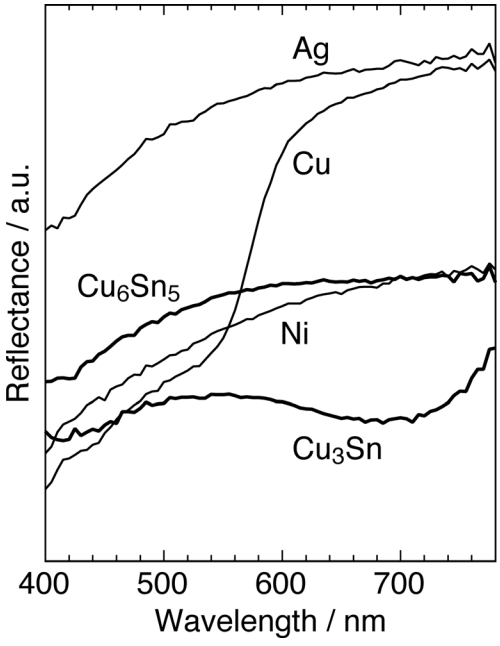

Figure 10. Visible reflection spectra of single-phase Cu_6Sn_5 and Cu_3Sn layers prepared by the alloying of Cu layer at + 5 and + 20 mV *vs.* Sn rod, respectively, using EMI-Tf_2N bath containing 0.05 mol dm^{-3} $Sn(Tf_2N)_2$ at 150°C. The spectra of Ni, Cu, and Ag are also depicted.

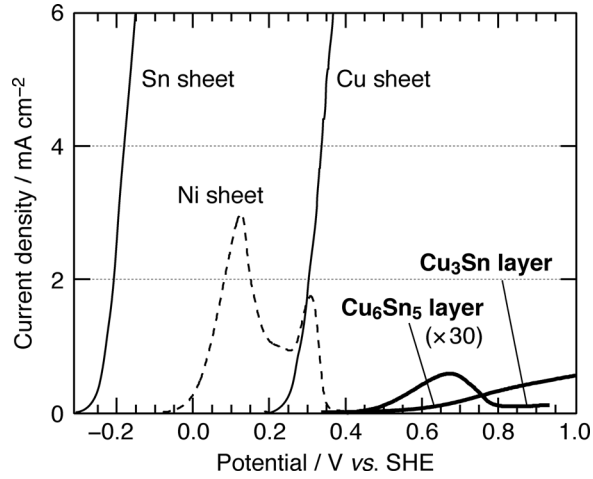

Figure 11. A set of typical anodic polarization curves for the same single-phase Cu_6Sn_5 and Cu_3Sn layers as in Fig. 10 immersed in 0.05 mol dm^{-3} H_2SO_4 aqueous solution. The curves for pure Ni, Cu, and Sn electrodes are also shown. Scan rate was 0.5 mV s^{-1} for all samples.

If it is to be used as an alternative to Ni underplating, knowledge of the corrosion behavior of a Cu-Sn layer will be of importance. Figure 11 shows a set of anodic polarization curves for the single-phase Cu_6Sn_5 and Cu_3Sn layers obtained in diluted sulfuric acid (50 mmol dm^{-3} H_2SO_4) at 25°C. Here, the potential was measured with a Ag/AgCl (3.33 mol dm^{-3} KCl) reference electrode, and is quoted versus the standard hydrogen electrode (SHE). Corrosion potentials of Cu_6Sn_5 and Cu_3Sn were rather positive, + 403 and + 334 mV *vs.* SHE, respectively, and were higher than those of pure Ni (− 81 mV), Cu (+ 182 mV), and Sn (− 312 mV). When polarized positively from the corrosion potentials, the Cu_6Sn_5 and Cu_3Sn layers thoroughly passivated, whereas pure Cu and Sn readily dissolved anodically. Although Ni was also passivated, the observed critical current density for passivation was *ca.* 3 mA cm^{-2}, which was

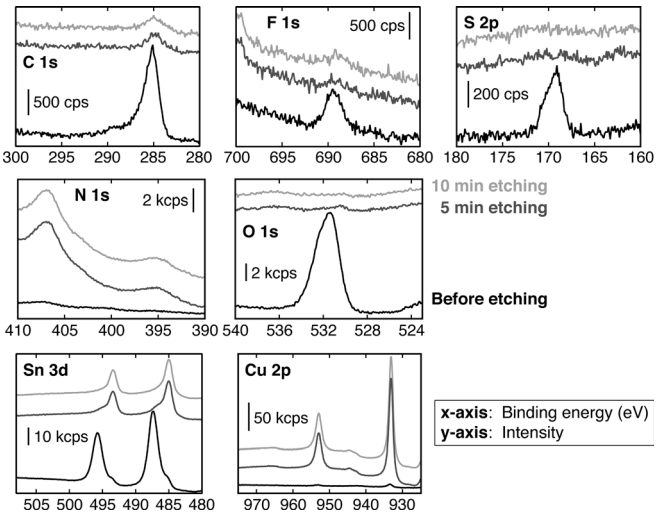

Figure 12. X-ray photoelectron spectra of Cu_6Sn_5 layer before and after Ar-ion etching for 5 and 10 min. The Cu-Sn layer was prepared by galvanic contact alloying of Cu sheet for 72 h at 150°C using EMI-Tf_2N bath containing 0.05 mol dm^{-3} $Sn(Tf_2N)_2$.

higher than those for Cu_6Sn_5 and Cu_3Sn layers. Figure 12 summarizes the XPS spectra for the Cu-Sn layer. According to the spectra acquired before Ar-ion etching, the surface of the layer is contaminated with C, F, S, and O, which are derived from EMI-Tf_2N. In contrast, these elements, except for a trace of carbon, were not detected after etching for 5–10 min, which corresponds to 20–40 nm in terms of SiO_2 thickness, suggesting that the non-faradaic inclusion of solute and/or solvent, *i.e.* EMI-Tf_2N here, hardly takes place, unlike the cases of conventional alloy electrodeposition. This is one important feature of alloying using the RD method. In addition, the XPS spectra indicate the alloy surface to be covered with an almost Cu-free SnO_x layer, which might be related to the corrosion resistance of the Cu-Sn alloy. On the other hand, the residual ionic liquid on the surface may improve the corrosion behavior. However, it seems less likely since Cu-Sn speculum layers prepared from aqueous alloy electrodeposition[14] also show similar corrosion resistance.

Conclusions

In the present study, Cu thin layer electroless deposition on a heat-resistant high-T_g glass epoxy substrate was attempted for use as a Cu substrate for reduction-diffusion (RD) alloying in an ionic liquid-based bath containing Sn^{2+} ions at 150°C. The part of the Cu layer immersed into the alloying bath was converted to a compact and adhesive silver-white Cu-Sn "speculum alloy" layer composed of intermetallic phases, Cu_6Sn_5 and/or Cu_3Sn. As a result, we demonstrated the first alloy metallization of a non-conductive polymer substrate through successive electrochemical deposition using two baths, each containing different metal ions, *i.e.* Cu^{2+} and Sn^{2+}. The abundance of the two Cu-Sn intermetallic phases could easily be controlled by an appropriate choice of applied potential and alloying time, in which a Sn reference electrode played a significant role for stable process operation. Taking advantage of the potential-dependent alloying process, the color and anodic behavior, which are important properties of the Cu-Sn layer as an alternative to nickel undercoating, were compared between single-phase Cu_6Sn_5 and Cu_3Sn. While both the phases exhibited passivation behaviors like nickel in diluted H_2SO_4 solution, they had different color shades, *i.e.* white-silver and bluish silver, respectively, and it was found that the color of the Cu_6Sn_5 was more appropriate as a nickel substitute.

The nonvolatile and nonflammable ionic liquid solvents were tailored for the present RD alloying. Aqueous baths cannot be used at 150°C without a pressure-tight vessel. Organic solvent-based baths, if any, are volatile and flammable, making the working conditions of electroplaters hazardous. Baths using high temperature molten salts generally require a glove box to avoid moisture. Most of the studies on electrodeposition using ionic liquids take advantage of their wide electrochemical window. In contrast, the target element of the present research, *i.e.* Sn, is a metal that can electrodeposit from aqueous baths. Therefore, the RD process offers a new type of application for ionic liquids in this field, using their nonvolatile and nonflammable natures at medium-low temperatures while ignoring the nature of the wide electrochemical window. In this study, however, we cheated a little in selecting the polymer substrate for initial copper electroless deposition. We prepared the polymer substrate with a roughened surface by dissolving away the Cu layer of commercially available copper foil-clad laminate, so in this sense it is not surprising that the resulting Cu-Sn layers had a good adhesiveness. This procedure was a temporary expedient to get a roughened epoxy substrate for various experiments, but is of course not realistic for practical processes. On the other hand, as far as we know, a convenient roughening procedure for epoxy substrates has not yet been established, unlike the case of ABS resin. Studies on chemical/physical etching of epoxy substrate are currently underway in our group.

Acknowledgments

This work was partially supported by a Grant-in-Aid for Scientific Research (no. 21360369) from the Japan Society for the Promotion of Science (JSPS) and Kyoto University Global COE Program, "International Center for Integrated Research and Advanced Education in Materials Science" from the Ministry of Education, Culture, Sports, Science, and Technology of Japan.

Kyoto University assisted in meeting the publication costs of this article.

References

1. A. Brenner, *Electrodeposition of Alloys — Principles and Practice*, Vol. 1, p. 7, Academic, New York (1963).
2. T. Katase, R. Kurosaki, K. Murase, T. Hirato, and Y. Awakura, *Electrochem. Solid-State Lett.*, **9**, C69 (2006).
3. K. Murase, R. Kurosaki, T. Katase, H. Sugimura, T. Hirato, and Y. Awakura, *J. Electrochem. Soc.*, **154**, D612 (2007).
4. A. Ito, K. Murase, T. Ichii, and H. Sugimura, *Electrochemistry*, **77**, 677 (2009).
5. K. Murase, A. Ito, and H. Sugimura, *ECS Trans.*, **11**(28), 103 (2008).
6. N. Tachikawa, N. Serizawa, Y. Katayama, and T. Miura, *Electrochim. Acta*, **53**, 6530 (2008).
7. Electrodeposition from Ionic Liquids, F. Endres, A. P. Abbott, and D. R. MacFarlane, Editors, p. 296, Wiley-VCH Verlag, Weinheim (2008).
8. K. Murase, K. Nitta, T. Hirato, and Y. Awakura, *J. Appl. Electrochem.*, **31**, 1089 (2001).
9. T. Katase, K. Murase, T. Hirato, and Y. Awakura, *J. Appl. Electrochem.*, **37**, 339 (2006).
10. K. Murase and Y. Awakura, *Trans. Mater. Res. Soc. Jpn.*, **29**(1), 55 (2004).
11. B. C. M. Martindale, S. E. Ward Jones, and R. G. Compton, *Phys. Chem. Chem. Phys.*, **12**, 1827 (2010).
12. N. Saunders and A. P. Miodownik, in Phase Diagrams of Binary Copper Alloys, P. R. Subramanian, D. J. Chakrabarti, and D. E. Laughlin, Editors, Monograph Series on Alloy Phase Diagrams 10, p. 412, ASM International, Materials Park, OH (1994).
13. J.-H. Shim, C.-S. Oh, B.-J. Lee, and D. N. Lee, *Z. Metallkd.*, **87**, 205 (1996).
14. T. Nakamura, Y. Mizutani, T. Nagayama, N. Shinohara, and H. Nawafune, *Hyomen Gijutsu*, **55**, 484 (2004).